energies

MDPI

Article

Hybrid-Domain Evaluation PTS with Adaptive Selection Methods for PAPR Reduction

Feng Hu [1], Yuan Lu [1,*], Libiao Jin [1], Jianbo Liu [1], Zhiping Xia [2], Guoting Zhang [2] and Jingting Xiao [2]

[1] School of Information and Communication Engineering, Communication University of China, Beijing 100024, China; fenghu@cuc.edu.cn (F.H.); libiao@cuc.edu.cn (L.J.); ljb@cuc.edu.cn (J.L.)
[2] Academy of Broadcasting Science, Beijing 100045, China; xiazhiping@abs.ac.cn (Z.X.); zhangguoting@abs.ac.cn (G.Z.); xiaojingting@abs.ac.cn (J.X.)
* Correspondence: luyuancuc@cuc.edu.cn

Abstract: The partial transmit sequence (PTS) technique is a fairly suitable scheme to mitigate the high peak-to-average power ratio (PAPR) problem inherent in 5G multicarrier systems, especially considering a high-order QAM modulation design. However, the high computational complexity level and the speed of the convergence for optimizing the phases of the transmitting signal restrict this technique in practical applications. In this paper, a low-complexity frequency-domain-evaluated PTS (F-PTS) based on a spacing multiobjective (SMO) processing algorithm is proposed to reduce the PAPR values. The PAPR performance are accurately predicted in terms of modifying relative dispersion in the frequency domain. As a result, the complexity of searching the optimal phase factors and IFFT computing is simplified. Moreover, a frequency-domain- and time-domain-evaluating PTS (FTD-PTS) is employed to search the optimal solution with a reasonable complexity. Simulation results verify that the operation rate of F-PTS is significantly improved after transferring the exhaustive search strategy of PTS into the SMO algorithm, and the F-PTS PAPR reduction performance is just 0.3 dB away from theoretical optimal performance. The FTD-PTS spends an acceptable operation rate to obtain optimal PAPR reduction performance, which subtracts 0.5 and 0.6 dB more than PSO-PTS and conventional PTS at CCDF $= 10^{-3}$, respectively.

Keywords: multicarrier system; 5G communication; partial transmission sequence; OFDM; power amplifier efficiency; PAPR

Citation: Hu, F.; Lu, Y.; Jin, L.; Liu, J.; Xia, Z.; Zhang, G.; Xiao, J. Hybrid-Domain Evaluation PTS with Adaptive Selection Methods for PAPR Reduction. *Energies* **2022**, *15*, 2738. https://doi.org/10.3390/en15082738

Academic Editor: KHANDAKAR AHMED

Received: 10 March 2022
Accepted: 7 April 2022
Published: 8 April 2022

1. Introduction

Recently introduced 5G communication systems can be applied in enhanced mobile broadband (eMBB), ultrareliable and low-latency communication (URLLC), massive machine type communication (mMTC) scenarios [1]. The multicarrier system is one of the critical technologies of 5G, which improves the spectral efficiency of 5G. Orthogonal frequency division multiplexing (OFDM) is one of the most representative multicarrier modulation (MCM) techniques due to its capability to efficiently cope with frequency-selective channels for 5G broadband wireless communication [2]. In addition, OFDM is applied in various communication systems [3]. Japan has developed the Integrated Service Digital Broadcasting-Terrestrial (ISDBT) [4] standard; China has developed the Digital Television Multimedia Broadcasting (DTMBH) [5] standard. Due to the anti-multipath fading characteristic of OFDM, OFDM is applied in various IEEE physical layer [6] name protocols in WLAN . However, OFDM is restricted by obstacles such as the high peak-to-average-power ratio (PAPR) [7], which drives the OFDM signals to work in the nonlinear region of high-power amplifiers (HPA) [8] and this leads to the appearance of an undesirable degradation in the bit error rate (BER) [9] performance. An increase in the back-off of HPA will lead to a loss in power efficiency; therefore, PAPR reduction is necessary and more efficient for energy optimization.

Various PAPR reduction schemes have been proposed to solve this issue, including signal distortion, coding and probability schemes. As a distortion technology, the clipping scheme [10] reduces PAPR by clipping the peak signal, but it produces additional noise and distortion to the system. Coding technology [11] encodes the signal without distortion and transmits signals with the lowest PAPR, increasing signal redundancy and reducing spectral efficiency. Probability technologies include particle sequence selection (PTS) [12], selective mapping (SLM) [13], tone reservation (TR) [14] and tone injection (TI) [15] technologies, which reduce PAPR by changing phase factors without distortion. A comparison of PAPR reduction schemes is given in Table 1. Among all existing techniques, PTS is very promising for a 5G waveform because of its efficient PAPR reduction performance without any signal distortion. The major drawback of PTS technologies is high computational complexity. To search for the optimal phase combination, large numbers of sub-blocks are inevitable, which increases the searching complexity exponentially [16]. In low-complexity PTS methods, one of the most attractive methods is using dominant time-domain samples. Unfortunately, a set of multipoint IFFT operations using entire points is required to calculate PAPR values, which significantly increases computational complexity, especially for the PTS algorithm.

Table 1. List of PAPR reduction schemes comparisons.

	Distortionless	**Power Increase**	**Implementation Complexity**	**High-Order-QAM Fitness**
Clipping	No	No	Low	Low
Coding	Yes	No	Low	Low
PTS/SLM	Yes	No	High	High
TR/TI	Yes	Yes	High	High

Various schemes have been proposed to improve PTS techniques. The pseudo-random and interleaving segmentation PTS method (PR-IL-PTS) [17] applied adjacent and random joint segmentation to improve PAPR reduction performance with a lower computational complexity, but the effect of the PAPR reduction was not satisfactory. The real and imaginary parts PTS method (RI-PTS) [18] dispersed the signal's real and imaginary phase factors, respectively, which improves the PAPR reduction performance but increases the computational complexity. The particle swarm optimization algorithm (PSO) PTS method refers to the phase factor as particles, employs the iterative function to update the particle position iteratively and acquires the best combination of phase factors by particle mutual learning. However, the computational complexity of PSO-PTS rises sharply with the number of iterations. Ref. [19] applied discrete Fourier transform to improve the PAPR reduction performance with considerable computational complexity.

In this work, a new metric which can select dominant frequency-domain samples accurately is proposed. Specifically, we propose a novel method based on a spacing multiobjective (SMO) processing algorithm to search for a suboptimal PTS scrambling signal [20]. The PAPR performance is accurately predicted in terms of modifying the relative dispersion before the IFFT operations. Then, the dominant complexity of computing the IFFT is evaded. The proposed low-complexity F-PTS methods can achieve much lower computational complexity without degrading the PAPR reduction performance. We also show that SMO processing has a unique structure that can be exploited to implement the PTS efficiently. Thus, the second proposed scheme, FTD-PTS, may achieve an optimal solution within a faster convergence speed. An evaluation of SMO is conducted to favor a PTS subset before the IFFT operations, instead of randomly selecting a subset. Then, time-domain metrics are used to estimate the PAPR of each candidate signal after finding the preferred PTS subset. Then, time-domain metrics are used to estimate and designate the achievable optimal solution accurately and remove parts of the samples from the procedure of the preferred PTS subset. Compared with the conventional PTS method, the improved

PTS method has a reasonable computational complexity and PAPR reduction can reach achievable lower bounds accurately.

To sum up, PTS and its improved versions have issues with high computational complexity or relatively poor PAPR reduction performance. This research proposes two advanced PTS algorithms (F-PTS and FTD-PTS) to reduce the computational complexity and achieve an optimal PAPR reduction performance with reasonable computational complexity.

This paper is arranged as follows. Section 2 explains the OFDM system and its inherent PAPR issue. Section 3 introduces the conventional PTS scheme and analyzes its computational complexity. Section 4, exploring the relationship between the PTS signals correlation and PAPR, proposes a low-computational-complexity F-PTS scheme based on a multiobjective optimization algorithm. Section 5 improves the F-PTS algorithm and proposes a FTD-PTS algorithm based on the time- and frequency-domain joint evaluation algorithm, which achieves the best PAPR reduction performance within an acceptable computational complexity. Section 6 presents the simulation results of F-PTS and FTD-PTS.

2. OFDM System

In this section, the OFDM structure and PAPR definition are presented. The continuous-time baseband OFDM sequence can be expressed as:

$$x(t) = \sum_{k=0}^{N-1} X_k(t) e^{j2\pi k \Delta f t}, 0 \le t \le T \tag{1}$$

where N data symbols $\mathbf{X} = \{X_k, k = 0, 1, \ldots, N-1\}$ generate the OFDM signals, which are chosen from phase-shift-keying (PSK) or quadrature amplitude modulation (QAM) constellation mapping, T represents the OFDM signal duration and $\Delta f = 1/T$ is the frequency interval between subcarriers [21].

Likewise, the discrete-time baseband OFDM sequence with L-time oversampling can be represented as:

$$x_n = \frac{1}{\sqrt{LN}} \sum_{k=0}^{N-1} X_k(t) e^{j2\pi nk/LN}, \; n{=}0, 1, \ldots, LN-1 \tag{2}$$

According to the central limit theorem, OFDM signals with massive subcarriers follow a Gaussian distribution, whose amplitude follows a Rayleigh distribution. The peak-to-average power ratio (PAPR) is usually used to describe the characteristics of signal amplitude fluctuations, which occur when different phase subcarriers achieve the maximum amplitude simultaneously [22]. A high PAPR will lead to HPA exceeding the dynamic range, causing nonlinear distortion. The PAPR of an L-time-oversampled OFDM signal can be defined as:

$$\mathrm{PAPR} = 10\log_{10}\left(\frac{\max\limits_{0 \le n \le NL-1}\left[|x_n|^2\right]}{\underset{P_{av}x(n)}{\mathrm{E}\left[|x_n|^2\right]}}\right) \tag{3}$$

The complementary cumulative distribution function (CCDF) is the major measure instrument to clarify the performance of PAPR in OFDM systems, which is defined as the probability that the PAPR exceeds a certain threshold Z_0 [23].

$$\begin{aligned} &\mathrm{CCDF}_{PAPR}(\mathrm{PAPR}_0) = \Pr(\mathrm{PAPR} > \mathrm{PAPR}_0) \\ &= 1 - \mathrm{F}(Z) \\ &= 1 - (1 - \mathrm{e}^{-Z_0})^N \end{aligned} \tag{4}$$

3. PTS Technique

A high PAPR is a major obstacle to the high energy efficiency of MCM systems in 5G communications [24]. Via continuous signal sub-blocks and computational power consumption, PTS is a nondistortion method and one of the few PAPR reduction techniques that applies in 5G high-order QAM communication scenarios [25].

3.1. PTS Scheme

The principle of PTS is to reduce PAPR by scrambling partitioned sub-blocks into different phases. Figure 1 depicts the scheme of PTS, where the input frequency-domain signal was divided into several subcarriers, each of them was conducted with an IFFT and scrambled with phase factors, then the signals in the time-domain with the minimum PAPR were chosen [26].

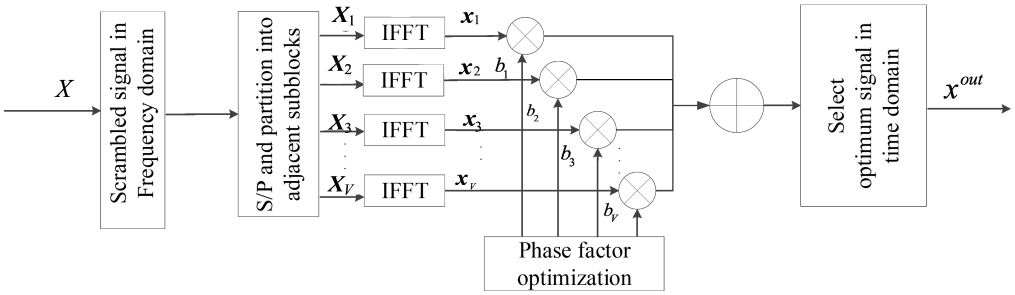

Figure 1. The structure of PTS system.

The main algorithm of the PTS scheme is shown in Figure 2. A frequency-domain signal $\mathbf{X}$ is divided into V disjoint sub-blocks as $\boldsymbol{X}_v = [X_{v,0}, X_{v,1}, \ldots, X_{v,N-1}]$, and $v = \{1, 2, \ldots, V\}$, where only N/V signals are available while others are padded with 0. A random OFDM signal can be shown as follows:

$$X_v(k) = \begin{cases} X(k), if X(k) \subseteq X_v \\ 0, if X(k) \not\subset X_v \end{cases} \tag{5}$$

where $X(k)$ denotes a signal appearing in the vth sub-block. The phase weighting factors $\boldsymbol{b} = [b_1, b_2, \ldots, b_V]$ are achieved by $\Phi = \left\{e^{j\phi_1}, \ldots, e^{j\phi_v}, \ldots, e^{j\phi_V}\right\}$, where
$\varphi_\omega \in [0, 2\pi)$, which can be represented as:

$$\mathbf{b} = \left\{b_v = e^{j2\pi v/V} | v = 0, 1, \ldots\ldots, V-1\right\} \tag{6}$$

Thus, the scrambled serial time-domain signal can be written as:

$$\mathbf{x} = \text{IFFT}\left\{\sum_{v=1}^{V} b_v \mathbf{X}_v\right\} = \sum_{v=1}^{V} b_v \mathbf{x}_v \tag{7}$$

where $\boldsymbol{x_v} = \boldsymbol{F}_v^{-1}\boldsymbol{X_v}$ is the candidate signal in the time domain and $\boldsymbol{F}_v^{-1}$ is the IFFT calculation padded with 0. Basically, PTS utilizes random phase factors to disperse the phase distribution, so that a high PAPR can be avoided.

Finally, the optimum phase factors combination with minimum PAPR are chosen as follows:

$$\begin{aligned} \boldsymbol{b}_{\text{opt}} &= \underset{\mathbf{b}_k}{\text{argmin}} \left(\max_{0 \le n \le NL-1} \left| \sum_{v=1}^{V} b_v \cdot x_v \right| \right) \\ \text{s.t. } \boldsymbol{b}_k &= [b_1, b_2, \ldots, b_v],\ k = 1, \ldots, M \end{aligned} \tag{8}$$

where b_{opt} is the best combination. $V!$ groups of none-repeating candidate signals can be generated and M groups of candidate signals are randomly selected from $V!$. The closer M is to $V!$, the closer the probability is to the theoretical best phase factors combinations.

To demodulate the signals at the receiver, side information (SI) about the phase rotation factors must be sent as well; the quantity of SI can be represented as: $\text{SI}^{\text{C-PTS}} = \log_2 V!$ BS, where BS is bits per sample.

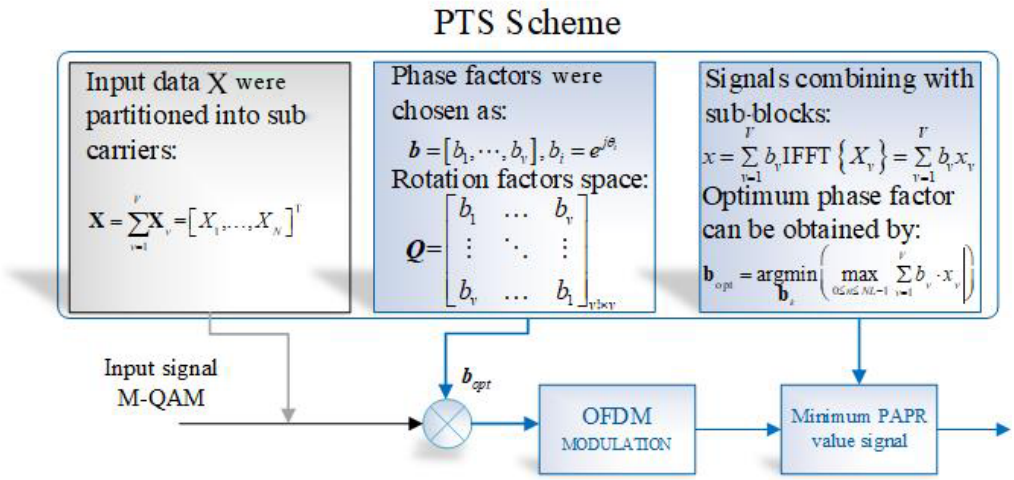

Figure 2. The algorithm of PTS system.

3.2. Computational Complexity and Optimization of PTS

It is well-known that conventional PTS scheme has an extremely high computational complexity when exhaustively searched. Particularly, the massive IFFT calculation is an insupportable burden [27].

The complexity of random partitioning PTS when applying the LN-FFT calculation can be represented as:

$$C_{add} = V(LN\log_2 LN) \tag{9}$$

and

$$C_{mult} = V(\frac{LN}{2}\log_2 LN), \tag{10}$$

respectively, where C_{add} represents the additive computational complexity and C_{mult} represents the multiplicative computational complexity.

The complexity of PTS when applying M searching spaces in (8) can be represented as:

$$CS_{add} = MLN(V-1) \tag{11}$$

and,

$$CS_{mult} = MLN(V+1) \tag{12}$$

It can be concluded from (11) and (12) that the complexity increases exponentially with the increase in the searching time M.

4. Low-Computational-Complexity F-PTS

Simply put, PAPR is due to the superposition of the peak amplitudes in the adjacent subcarriers, which produces a resonance like effect; it can be inferred that a frequency-domain phase-discretization technique would exist to reduce the probability of PAPR generation.

For evaluating dispersion, the difference in correlation R_{ab} between rotation factors is analyzed in this section. Assuming that $x_{v,n}$ from $\mathbf{x_v} = [x_{v,0}, x_{v,1}, \ldots, x_{v,n}, \ldots, x_{v,N-1}]^{\mathrm{T}}$ is a sequence of independent complex numbers following $N(0, \sigma^2/2V)$. The correlation among two random signals can be represented as:

$$R_{ab}\left(x_a^{'}(m), x_b^{'}(n)\right) = \frac{1}{N}\left(\sum_{k=0}^{N-1}\sum_{y=0}^{N-1} b_i^k b_l^{y^*} X'(k)X'(y)^* \exp\left(j\frac{2\pi(km-yn)}{N}\right)\right)$$
$$,1 \le i,l \le U; 0 \le m,n < N \tag{13}$$

where $x_a^{'}(m)$ and $x_b^{'}(n)$ [28] represent two random signals and $X'(k)$, $X'(y)$ represent corresponding frequency-domain signals. Defining $\tau = m - n$, after simplification, (13) can be written as:

$$R_{ab}\left(x_a^{'}(m), x_b^{'}(n)\right) = \frac{1}{N}\sum_{v=1}^{V} b_i^v b_l^{v^*} \sum_{k\in\vartheta_v} \exp\left(j\frac{2\pi k\tau}{N}\right), -N < \tau < N \tag{14}$$

Substituting a random partitioned standard $\Phi_v = \{P \text{ random independent subcarriers}\}$ and defining the correlation of two random signals as $R_{R,ab}(\tau)$, (14) can be transformed into :

$$\left|R_{R,ab}(\tau)\right| \approx \begin{cases} 0 & ,\tau \neq 0 \\ \frac{1}{V}\cdot\left|\sum_{v=1}^{V} b_i^v b_l^{v^*}\right| & ,\tau = 0. \end{cases} \tag{15}$$

When $\tau = 0$, the correlation of two random points in an identical signal can be evaluated applying (15) and the relationship of PAPR and $\left|R_{R,ab}(\tau)\right|$ is shown in Figure 3. In general, a scrambled signal with the highest PAPR is provided for reference when the correlation is one; the PAPR increases with the rise of $\left|R_{R,ab}(\tau)\right|$. Since the positions of the high $\left|R_{R,ab}(\tau)\right|$ signal's high-amplitude are centralized, a high PAPR is inevitable. Low $\left|R_{R,ab}(\tau)\right|$ can be obtained by increasing the dispersion of phase factors. We assumed that the highest PAPR signal was chosen, whose uncorrelation signal has a minimum PAPR, with a large $\left|R_{R,ab}(\tau)\right|$.

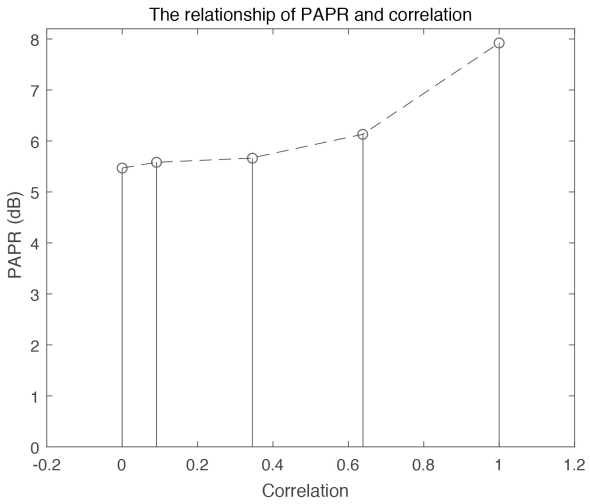

Figure 3. Amplitudes distribution of identical signal.

The above-mentioned analytical result can represent the correlation characteristic in the time domain only, to simplify the complexity of the PTS scheme, and the relationship of the PAPR and frequency domain signals are discussed in following contents. The correlation among two random signals $x_a^{'}$ and $x_b^{'}$ according to (16) can be represented as [28]:

$$\rho_{a,b} = \frac{\mathrm{cov}(x_a^{'}, x_b^{'})}{\sqrt{\mathrm{D}(x_a^{'})\mathrm{D}(x_b^{'})}} = \left(V - Q + \sum_{q=0}^{Q-1} S_q\right)\frac{1}{V} \tag{16}$$

where $v_q (q = 1, 2, \ldots, Q)$ represent two random signals. $x_a^{'}$ and $x_b^{'}$ occupy different phase factors which can be represented as:

$$\begin{cases} b_{v_q}^a \neq b_{v_q}^b \; if v_q = v_1, v_2, \ldots, v_q \\ b_{v_q}^a = b_{v_q}^b \; others \end{cases} \tag{17}$$

$\rho_{a,b}$ is described as the correlation between two random signals; therefore, the range of $\rho_{a,b}$ can be expressed as:

$$\rho_{a,b} \geq \frac{V - 2Q}{V}, \text{ for V} \geq 2Q \tag{18}$$

where the correlation of two candidate signals $\rho_{a,b}$ mainly depends on the variety Q. Thus, the maximum $\rho_{a,b}$ is obtained when $Q = 1$, which leads to the approximate PAPR.

In conclusion, the uncorrelation characteristic of the original signal $x_a^{'}$ and the scrambled signal $x_b^{'}$ is desirable, because the probability of a peak amplitude appearing in the same position in $x_a^{'}$ and in the scrambled signal $x_b^{'}$ can be minimized in this way.

In the F-PTS technique, dispersion in the frequency domain was evaluated by spacing multiobjective (SMO) optimization was adopted, and the candidate signal with the most dispersion phase factors was chosen.

MO optimization is widely used in various industries and has achieved remarkable success; it is aimed at finding the optimum solution among multiple objectives. Spacing multiobjective (SMO) optimization can tackle engineering problems and has been applied in F-PTS for evaluating phase factors dispersion [29].

Figure 4 illustrates the system model of the F-PTS scheme: signals were scrambled in the frequency domain, and the signal with the best phase factors dispersion was chosen by SMO and sent to the transmitter after the IFFT transmit. The operation of sub-blocks scrambling and partition can be described as:

$$\tilde{\mathbf{X}} = \sum_{v=1}^{V} b_v \cdot \mathbf{X}_v \tag{19}$$

where $\tilde{\mathbf{X}}$ are the frequency signals after scrambling. To achieve the maximum difference in the signal's correlation, SMO optimization is introduced, which can be represented as follows:

$$\begin{aligned} &N := e, \overline{X} := \bar{d}, X_i := d_i \\ &S = \sqrt{\frac{1}{N-1} \sum_{i=1}^{N} \left| \overline{X} - X_i \right|} \end{aligned} \tag{20}$$

where d_i is the plural form of significant points, $\bar{X}$ is the mean value of all points and X_i is the ith frequency signal from $\tilde{\mathbf{X}}$. When $S = 0$, the scrambled signals reach the most discrete state, the dispersion of the constellation gets worse with the increase of S. Therefore, the $V!$ combinations' dispersion can be examined as follows:

$$\begin{aligned} &\widetilde{\mathbf{b}}_{\text{opt}} = \underset{\mathbf{b}_k}{\text{argmin}} \left(\sqrt{\frac{1}{N-1} \sum_{i=1}^{N} \left| \overline{X} - X_i \right|} \right) \\ &\text{s.}t. \mathbf{b}_k = [b_1, b_2, \ldots, b_v] \\ &\text{s.}t. k = 1, \ldots, V! \end{aligned} \tag{21}$$

where $\widetilde{b}_{\text{opt}}$ is the scrambled signal combination with the best dispersion.

After applying the above method to evaluate the dispersion of the phase factors combination in the frequency domain, the signal with the most discrete phase factors can been transmitted, which can be expressed as:

$$\begin{aligned} \boldsymbol{x} &= \mathrm{IFFT}\{\boldsymbol{X}_{opt}\} \\ \boldsymbol{X}_{opt} &= \sum_{v=1}^{V} b_v \cdot \mathbf{X}_v \\ s.t.\ b &= b_{opt} \end{aligned} \tag{22}$$

where $\boldsymbol{X}_s$ is the most scrambled signal.

The F-PTS technique applied with a spacing algorithm can be described as Algorithm 1.

Algorithm 1 F-PTS with low computational complexity

Input: OFDM signal in the frequency domain

Output: OFDM signal in the time domain with the compromise optimal PAPR reduction performance

Begin
Initialize the data of the OFDM system
Generate $V!$ groups of phase factors combinations as $\boldsymbol{b}_{v!}$
for $n = 1:1:N$ **do**
    Partition the OFDM signal as: $\mathbf{X} = \sum_{v=1}^{V} b_v \mathbf{X}_v$
    for $v = 1:1:V$ **do**
        Apply the adjacent partition method
    end for;
end for;

function MERGER($V!, x$)
    for $i = 1:1:V!$ **do**
        Scramble the signals as: $\mathbf{X} = \sum_{v=1}^{V} b_v X_v$
        Evaluate the frequency-domain signal dispersion as:
    $Spacing(X_i) = \sqrt{\frac{1}{N-1}} \sum_{i=1}^{N} |\bar{X} - X_i|$
    end for
    Select the signal with the best dispersion:$x_{opt} = \sum_{v=1}^{V} b_v \cdot x_v = \sum_{v=1}^{V} b_v \cdot \mathrm{IFFT}\{X_v\}$
    Compute the per se signal PAPR as result
    return *result*
end function$\widetilde{\mathbf{b}}_{\mathrm{opt}} = \underset{\mathbf{b}_k}{\operatorname{argmin}} \left(\sqrt{\frac{1}{N-1}} \sum_{i=1}^{N} \left| \overline{X} - X_i \right| \right) \mathrm{s}.t. \mathbf{b}_k = [b_1, b_2, \ldots, b_v]\, \mathrm{s}.t.\ k = 1, \ldots, V!$
F-PTS achieves suboptimal PAPR reduction performance and outputs an OFDM signal with low PAPR.
End

The algorithm and structure of the F-PTS system are shown in Figures 4 and 5, where F-T indicates frequency domain.

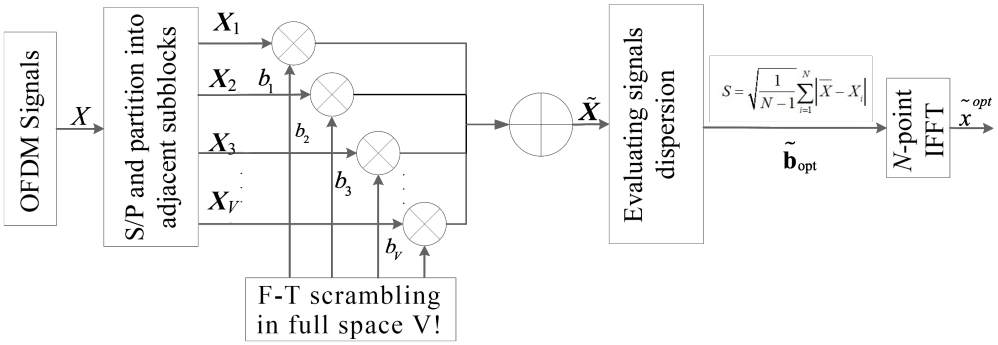

Figure 4. Structure of the F-PTS system.

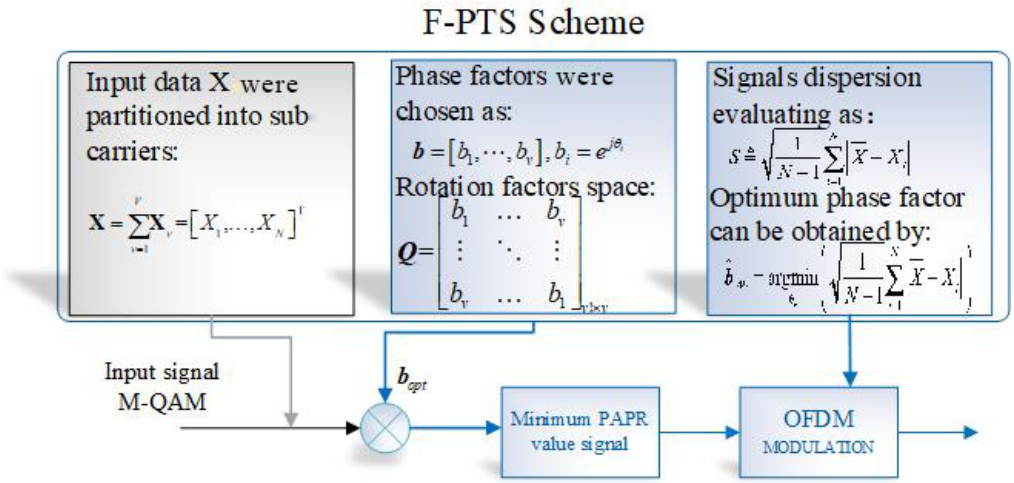

Figure 5. Algorithm of the F-PTS system.

The complexity of the F-PTS technique with the SMO algorithm can be represented as:

$$C_{f-add} = LN \cdot \log_2 LN + (V-1)V!\frac{N}{V} + V![2\mathrm{O}(N)] \tag{23}$$

and,

$$C_{f-mult} = V!\mathrm{O}(N^2) + (LN/2)\log_2 LN \tag{24}$$

where $g_o = V![2\mathrm{O}(N)+\mathrm{O}(N^2)]$ is the complexity of the SMO algorithm, the addition and subtraction operations are both $\mathrm{O}(N)$ and the quadratic operation is $\mathrm{O}(N^2)$.

Signals with higher frequency-domain dispersion performance have a lower probability to produce high PAPR, which is considered as a suboptimal algorithm.

The proposed F-PTS scheme first chooses the scrambled signal with the highest frequency dispersion, then avoids massive IFFT calculation complexity. Since the peak amplitude superimposition can be avoided by evaluating dispersion, only one IFFT is required and a compromise performance can be obtained by the F-PTS technique. As a result, the complexity is dramatically reduced.

5. Frequency-Domain and Time-Domain Evaluation of the PTS (FTD-PTS) Method

The proposed FTD-PTS scheme aims to find the optimal solution with a reasonable computational complexity.

To further explore whether PAPR is only affected by $\boldsymbol{b} = [b_1, b_2, \ldots, b_V]$, the mth candidate signal can be expressed as:

$$\boldsymbol{x}_m = \sum_{v=1}^{V} b_v x_{v,m},\ m=0,1,\ldots,M\text{-}1 \tag{25}$$

so that the power of signal $\mathbf{x}_m$ can be described as:

$$\begin{aligned} |x_m^c|^2 &= \left|\sum_{v=1}^{V} b_v^c x_{v,m}\right|^2 = \left(\sum_{v=1}^{V} b_v^c x_{v,m}\right)\left(\sum_{v=1}^{V} b_v^c x_{v,m}\right)^* \\ &= \underbrace{\sum_{v=1}^{V} |x_{v,m}|^2}_{\mathbf{Q}_m} + \underbrace{\sum_{v_1=1}^{V}\sum_{\substack{v_2=1 \\ v_1\neq v_2}}^{V} \left(b_{v_1}^c x_{v_1,m}\right)\left(b_{v_2}^c x_{v_2,m}\right)*}_{\mathbf{V}_m^c} \end{aligned} \tag{26}$$

where $\mathbf{Q}_m = \sum_{v=1}^{V} |x_{v,m}|^2$ and $\mathbf{V}_m^c = \sum_{v_1=1}^{V}\sum_{\substack{v_2=1 \\ v_1\neq v_2}}^{V} \left(b_{v_1}^c x_{v_1,m}\right)\left(b_{v_2}^c x_{v_2,m}\right)*$. $|x_m^c|^2$can be converted into the sum of $\mathbf{Q}_m$ and $\mathbf{V}_m^c$, so that (2) can be transformed as follows:

$$\mathrm{PAPR} = 10\log_{10}\left(\frac{\max[\mathbf{Q}_n + \mathbf{V}_m^c]}{\mathrm{E}\left[|x_n|^2\right]}\right) \tag{27}$$

Equation (27) shows that the rotation factors and amplitude affect the PAPR performance jointly.

The probability of F-PTS to choose the preferred PTS subject from the full space is much better than that of the conventional PTS. In other words, x_{opt} must have a good dispersion characteristic.

When only frequency-domain dispersion was considered in SMO, there was reduction of probability that high PAPR appears. A novel scheme applied in this section combined dispersion evaluation with affordable complexity, hope to obtain the optimal phase factors combination .

The FTD-PTS scheme is shown in Figure 6, where T-T indicates time domain; the frequency-domain dispersion evaluation is conducted before the time-domain one and Q groups included the preferred PTS subject are chosen more likely, instead of randomly selecting M groups. The optimal solution x_{opt} is exhaustively searched after finding the preferred PTS subject and is transformed into the time domain. By iteration, the minimum Q is obtained to ensure that $\mathbf{x}_{opt}$ could be chosen, and to minimize the computational complexity as much as possible.

The main steps of the FTD-PTS technique are described in Algorithm 2.

FTD-PTS method is illustrated in Figure 4. Initially, the input signals are partitioned and scrambled as follows:

$$\widehat{\mathbf{X}} = \sum_{v=1}^{V} b_v \cdot \mathbf{X}_v \tag{28}$$

where $\widehat{\mathbf{X}}$ is the generated candidate signals in the frequency domain. Then, the signals' dispersion is evaluated, and the preoptimization Q groups of high-dispersion candidate signals are as follows:

$$Spacing(\boldsymbol{X}_i) = \sqrt{\frac{1}{N-1}\sum_{i=1}^{N}\left|\overline{\widehat{X}} - \widehat{X}_i\right|} \tag{29}$$

$$[\mathbf{b}_1,\ldots,\mathbf{b}_Q] = \min \underset{k=1}{\overset{Q}{\mathrm{find}}} \left(\mathrm{Spacing}\left(\widehat{\mathbf{X}_k}\right)\right) \tag{30}$$

where $\widehat{\boldsymbol{X}}_i$ is the ith frequency-domain signal from $\widehat{\boldsymbol{X}}$. As the discrete center,

$\overline{\widehat{X}}$ is the mean value of all constellations. The dispersion performance gets worse with the increase of SMO.

Algorithm 2 FTD-PTS obtains optimum PAPR reduction performance with regular computational complexity

Input: OFDM signal in the frequency domain
Output: Minimize PAPR($\boldsymbol{b}$), subject to $\boldsymbol{b} \in \{\boldsymbol{b}_1, \boldsymbol{b}_2, \ldots, \boldsymbol{b}_v\}$

Begin
Initialize the data of the OFDM system
for $n = 1:1:N$ **do**
  Partition the OFDM signal as: $\widehat{\boldsymbol{X}} = \sum_{n=1}^{V-1} \mathbf{X}_V$
  for $v = 1:1:V$ **do**
    Apply the adjacent partition method
  end for;
end for;

function MERGER($V!, x$)
  for $i = 1:1:V!$ **do**
    Scramble signals as: $\overline{\boldsymbol{X}} = \sum_{v=1}^{V} b_v \cdot \mathbf{X}_v$
    Evaluate the frequency-domain signal dispersion as:
    $Spacing(\boldsymbol{X}_i) = \sqrt{\frac{1}{N-1}} \sum_{i=1}^{N} \left| \overline{\widehat{X}} - \widehat{X}_i \right|$
  end for
  for $n = 1:1:Q$ **do**
    Scramble the OFDM signal in the time domain as:
    $\widehat{\mathbf{x}} = \sum_{v=1}^{V} b_v \,\mathrm{IFFT}\left\{\widehat{\mathbf{X}}_v\right\} = \sum_{v=1}^{V} b_v \widehat{\mathbf{x}}_v,\ s.t.\ [b_1, b_2, \ldots, b_V] \in \left[\mathbf{b}_1, \ldots, \mathbf{b}_Q\right]$
  end for
  Select Q groups of preferred FTD-PTS subsets from the full space based on the SMO algorithm
  for $n = 1:1:Q$ **do** Search the optimal factor as:
  $\widehat{\mathbf{b}}_{\mathrm{opt}} = \underset{\mathbf{b}}{\mathrm{argmin}} \left(\max_{0 \le q \le Q} \left| \sum_{v=1}^{V} b_v \cdot \widehat{x}_v \right| \right),\ s.t.\ b_v \in [b_1, b_2, \ldots, b_V],\ s.t.\ [b_1, b_2, \ldots, b_V] \in \left[\mathbf{b}_1, \ldots, \mathbf{b}_Q\right]$
  end for
  Select Q groups of signals with the best dispersion $Q = 1$
  Select the best combinations from Q candidate signals as FTD's PAPR
  while $FTD - PAPR > C - PAPR$ **do**
    $Q = Q + 1$
    Select the best combinations from Q candidate signals as FTD's PAPR
  end while
  Output the minimum preselected space Q
  Compute the per se signal PAPR as result
  return *result*
end function
FTD-PTS achieves optimal PAPR reduction performance and outputs the OFDM signal with the lowest PAPR.
End

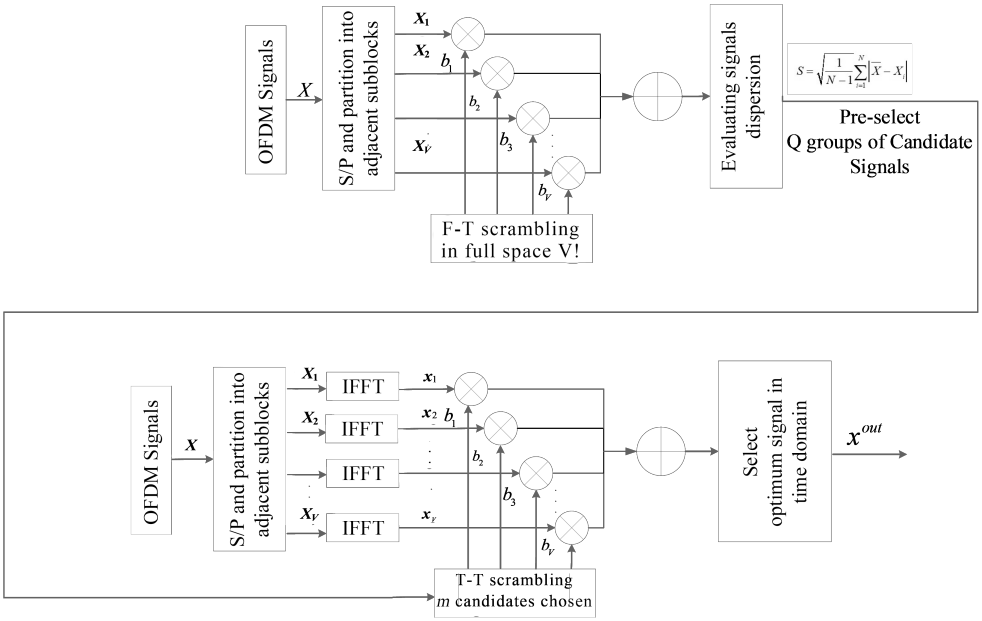

Figure 6. Structure of the FTD-PTS system.

Thirdly, Q groups of candidate signals are converted into disjoint sub-blocks and scrambled with phase factors after passing the IFFT blocks as follows:

$$\hat{\mathbf{X}} = \sum_{v=1}^{V} \widehat{\mathbf{X}}_v \tag{31}$$

$$\begin{aligned} &\widehat{\mathbf{x}} = \sum_{v=1}^{V} b_v \,\mathrm{IFFT}\left\{\widehat{\mathbf{X}}_v\right\} = \sum_{v=1}^{V} b_v \widehat{\mathbf{x}}_v \\ &s.t.\ [b_1, b_2, \ldots, b_V] \in \left[\mathbf{b}_1, \ldots, \mathbf{b}_Q\right] \end{aligned} \tag{32}$$

Finally, we search for the best combinations $\widehat{\mathbf{b}}_{\mathrm{opt}}$ from Q candidate signals. The experiment result shows that the statistical probability approaches stability when the sample space is large enough, which satisfies the principle of probability.

$$\begin{aligned} &\widehat{\mathbf{b}}_{\mathrm{opt}} = \underset{\mathbf{b}}{\mathrm{argmin}} \left(\max_{0 \le q \le Q} \left| \sum_{v=1}^{V} b_v \cdot \widehat{x}_v \right| \right) \\ &s.t.\ b_v \in [b_1, b_2, \ldots, b_V] \\ &s.t.\ [b_1, b_2, \ldots, b_V] \in \left[\mathbf{b}_1, \ldots, \mathbf{b}_Q\right] \end{aligned} \tag{33}$$

The flow chart of FTD-PTS can be seen in Figure 7; the minimum preiteration space Q can be obtained by feedback.

F-PTS only conducts one IFFT calculation, and utilizing the low-complexity frequency-domain dispersion evaluation instead of exhaustively searching in PTS achieves an extremely low complexity.

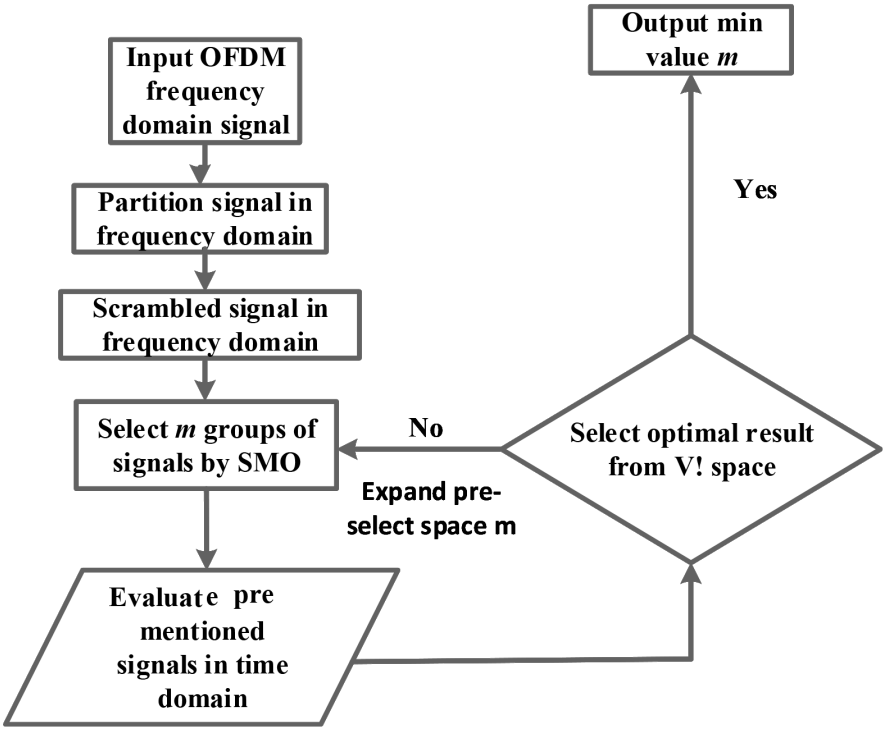

Figure 7. Flow chart of the FTD-PTS system.

FTD-PTS maintains an affordable system complexity, combining a frequency-domain evaluation and a search for Q best phase factors combinations to achieve a reasonable complexity.

The complexity of FTD-PTS can be described as:

$$\mathrm{C}_{FTD-add} = VLN\log_2 LN + (V-1)QLN + V![2\mathrm{O}(N)] \tag{34}$$

and,

$$\mathrm{C}_{FTD-mult} = V(LN/2)\cdot\log_2 LN + (V-1)V!\frac{N}{2} + V!\mathrm{O}(N^2) \tag{35}$$

where $\mathrm{C}_{FTD-add}$ and $\mathrm{C}_{FTD-mult}$ represent the additive and multiplicative complexities, respectively. FTD-PTS has the same approximate complexity as PTS.

Overall, the three techniques' computational complexity is mainly concentrated on the multiplier; F-PTS has the least complexity and FTD-PTS and PTS have a similar one as expressed in Table 2.

Table 2. The computational complexity of multiple PTS techniques.

PTS	Additive Complexity	Multiplicative Complexity
C-PTS	$V(LN/2)\cdot\log_2 LN$	$VLN\log_2 LN + (V-1)MLN$
F-PTS	$V!\mathrm{O}(N^2) + (LN/2)\log_2 LN$	$LN\cdot\log_2 LN + (V-1)V!\frac{N}{V} + V![2\mathrm{O}(N)]$
FTD-PTS	$V(LN/2)\cdot\log_2 LN + (V-1)V!\frac{N}{2} + V!\mathrm{O}(N^2)$	$VLN\log_2 LN + (V-1)QLN + V![2\mathrm{O}(N)]$

To provide a general understanding of all functions in this paper, this section separates all functions into three parts: conventional PTS, F-PTS and FTD-PTS. The overview of all functions is shown in Figure 8.

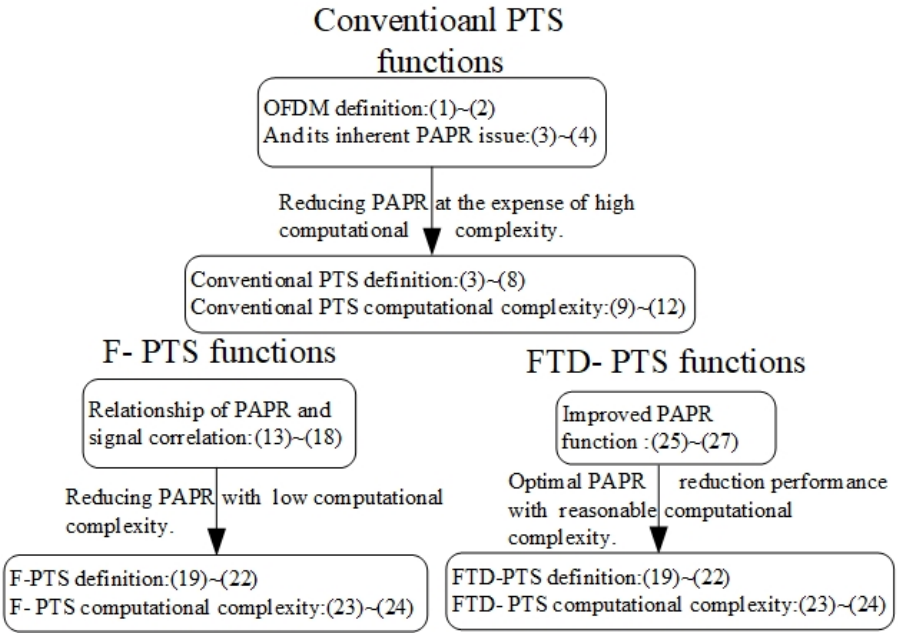

Figure 8. Overview of all functions introduced in this paper.

6. Simulation Results and Discussion

In this chapter, the PAPR reduction performance is shown for the proposed F-PTS and FTD-PTS schemes. Each OFDM signal was modulated by 64 QAM and 10^5 OFDM data blocks are generated. In F-PTS, the phase factors numbers were selected as $v = 6$, the phase partition numbers $W = V$ were the same as above, and we adopted a random partitioning method. The parameter setting of the FTD-PTS scheme was identical as that of the F-PTS scheme. All the simulations were completed in MATLAB. The parameters of the simulations are shown in Table 3.

Table 3. Simulations parameters.

Modulation System	OFDM
Total number of subcarriers (N)	1024
Number of oversampled (L)	4
Modulation method	64 QAM
Number of partitions (V)	6
Number of phase factors (W)	6
Partition method	Random

To demonstrate the relationship between complexity and PAPR reduction performance, Figure 9 compares the PTS performance with different candidate signals numbers. The exhaustive searching from PTS generates an extremely high computational complexity. For this issue, search was only performed M times. The comparison of the PTS performance with different M is shown as Figure 9; the PAPR reduction performance ascends when the number of sub-blocks is growing, because the probability of choosing the best combinations is growing.

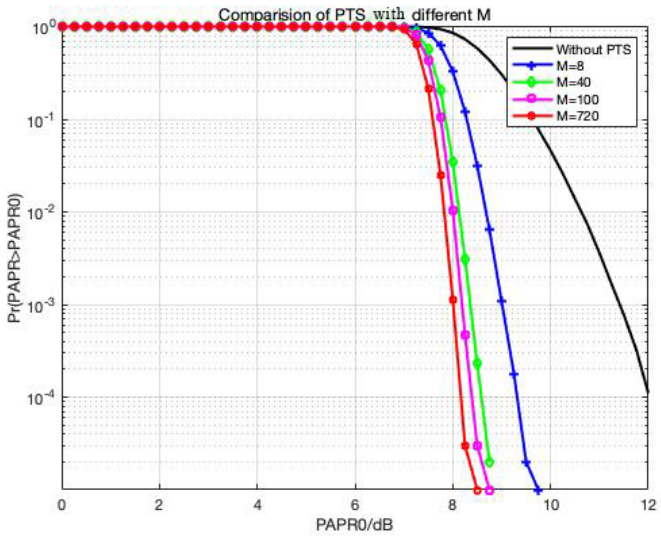

Figure 9. Comparison of PTS with different *M*.

6.1. F-PTS Simulation

F-PTS avoids the extensive IFFT and PAPR calculation workload and employs the SMO dispersion evaluation criterion to select the best dispersion scrambled frequency-domain signals. When CCDF $= 10^{-3}$, compared with the OFDM system, the conventional PTS, F-PTS and optimal PTS techniques reduce PAPR by 3 dB, 3.3 dB and 3.5 dB, respectively. Since the computational complexity of the SMO dispersion evaluation criterion is much lower than that of the IFFT and PAPR, F-PTS is a computational-complexity-friendly algorithm. The suboptimal performance can be obtained by applying dispersion as the evaluation criterion.

In Figure 10 and Table 4, we applied $W = V =$ six phase factors and generated 720 phase combinations. The PAPR reduction from best to worst are the optimal PTS scheme, which exhaustively searched the 720 phase combinations, F-PTS, which applied best dispersion phase combinations, PTS, which searched 32 phase combinations, and the OFDM system without PTS, with values of 7.9 dB, 8.1 dB, 8.3 dB and 11.2 dB, respectively, with CCDF = 10^{-3}. As shown in Figure 10, similar performance was obtained by optimal PTS and F-PTS. For example, optimal PTS and F-PTS had values of 8.0 dB and 8.2 dB for CCDF = 10^{-2}, respectively. In the meantime, F-PTS obtained an extremely low complexity. In conclusion, the performance of F-PTS is better than that of PTS when $m = 32$, and slightly inferior to that of PTS when $m = 720$, with extremely low complexity. The complexity of F-PTS was almost 50% of PTS.

Table 4. PAPR reduction performance of PTS and F-PTS.

PAPR Techniques	**PAPR at CCDF = e**		
	$e = 10^{-2}$	$e = 10^{-3}$	$e = 10^{-4}$
PTS with m = 32	8.2	8.3	8.4
F-PTS	8.0	8.1	-
PTS with m = 720	7.8	7.9	8.1

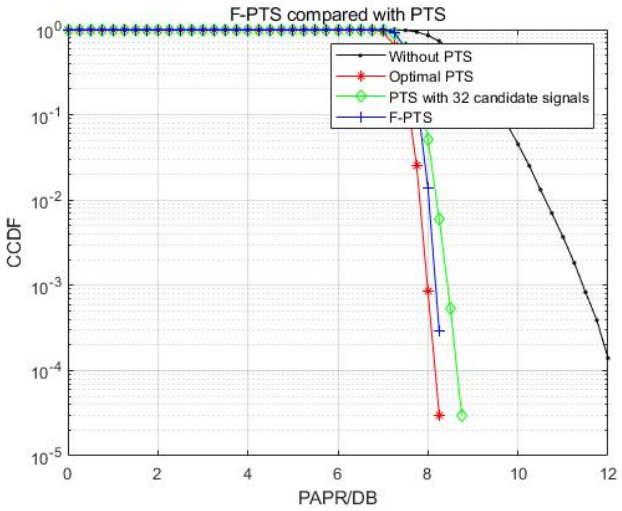

Figure 10. The comparison between performance of PTS and F-PTS.

6.2. FTD-PTS Simulations

F-PTS reduced computational complexity but failed to reach the optimal PAPR reduction performance. FTD-PTS is an enhanced version of F-PTS. It adopts the time- and frequency-domain joint evaluation algorithm to preselect the phase factors combinations containing the optimal solution, obtaining the optimal PAPR reduction performance with an acceptable calculation complexity.

In Figure 11 and Table 5, we applied $W = V =$ six phase factors and generated 720 phase combinations. The PAPR reduction performance comparison of FTD-PTS and conventional PTS when CCDF $= 10^{-3}$ is given in Table 6. When $Q = 4$, FTD-PTS and conventional PTS decreased PAPR by 3.0 dB and 2.0 dB, respectively, and FTD-PTS decreased PAPR by 1 dB more than conventional PTS; when $Q = 8$, FTD-PTS and conventional PTS decreased PAPR by 3.3 dB and 2.5 dB, respectively, and FTD-PTS decreased PAPR by 0.7 dB more than conventional PTS; when $Q = 32$, FTD-PTS and conventional PTS decreased PAPR by 3.6 dB and 3.1 dB, respectively, and FTD-PTS decreased PAPR by 0.5 dB more than conventional PTS; when $Q = 40$, FTD-PTS and conventional PTS decreased PAPR by 3.8 dB and 3.0 dB, respectively, and FTD-PTS decreased PAPR by 0.8 dB more than conventional PTS. Note that FTD-PTS reaches the optimal PAPR reduction performance when $Q = 40$. It can be concluded that FTD-PTS has a lower computational complexity than conventional PTS to achieve a better PAPR reduction performance.

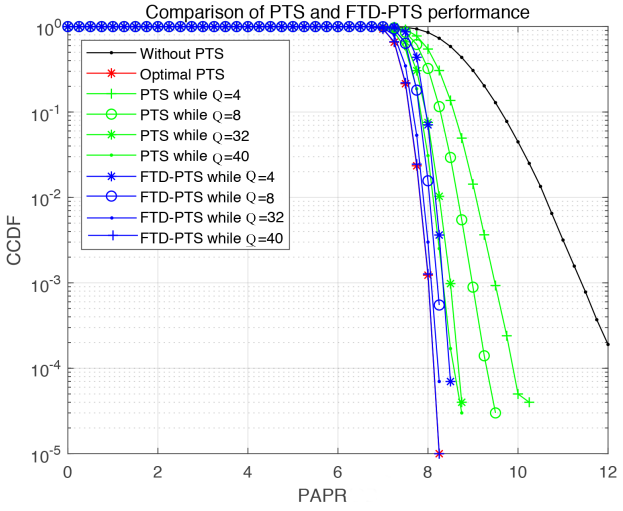

Figure 11. The performance comparison of FTD-PTS and PTS with different Q.

Table 5. PAPR reduction performance of PTS with different Q and FTD-PTS.

PAPR Techniques	PAPR at CCDF = e		
	$e = 10^{-2}$	$e = 10^{-3}$	$e = 10^{-4}$
PTS while Q = 4	8.5	8.6	8.9
PTS with Q = 8	8.25	8.5	8.8
PTS with Q = 32	8.1	8.2	8.3
PTS with Q = 40	7.9	8.0	8.25
FTD-PTS with Q = 4	8.05	8.2	8.25
FTD-PTS with Q = 8	8.0	8.1	-
FTD-PTS with Q = 32	7.85	7.95	8.17
FTD-PTS with Q = 40	7.8	7.9	8.1

Table 6. The PAPR reduction performance comparison of FTD-PTS and conventional PTS when CCDF $= 10^{-3}$.

PTS Schemes	PAPR Value When CCDF $= 10^{-3}$	PAPR Gain
Without PTS	11.5	0
FTD-PTS with Q = 4	8.5	3.0
FTD-PTS with Q = 8	8.2	3.3
FTD-PTS with Q = 32	7.9	3.6
FTD-PTS with Q = 40	7.7	3.8
PTS with Q = 4	9.5	2.0
PTS with Q = 8	9	2.5
PTS with Q = 32	8.4	3.1
PTS with Q = 40	8.3	3.2
Optimal PTS	7.7	3.8

To further represent the achievement of this paper, Figure 12 compares the PAPR reduction performance of conventional PTS, the FTD-PTS (with Q = 5, Q = 30 and Q = 40), and PSO-PTS (with iterations = 5, iterations = 30, iterations = 40). Because the particle velocity and position require an update in each iteration of PSO, the computational complexity of PSO-PTS rises sharply with the increase of the iterations. For a fair comparison, the alternative phase factor of FTD-PTS and PSO-PTS iterations are the same. The PAPR reduction performance comparison of FTD-PTS and PSO-PTS when CCDF $= 10^{-3}$ is given in Table 7. When $Q = It = 5$, FTD-PTS and PSO-PTS decreased PAPR by 3.2 dB and 2.6 dB, respectively, and FTD-PTS decreased PAPR by 0.6 dB more than PSO-PTS; when $Q = It = 30$, FTD-PTS and PSO-PTS decreased PAPR by 3.6 dB and 3.2 dB, respectively, and FTD-PTS decreased PAPR by 0.4 dB more than PSO-PTS; when $Q = It = 40$, FTD-PTS and PSO-PTS decreased PAPR by 3.8 dB and 3.3 dB, respectively, and FTD-PTS decreased PAPR by 0.5 dB more than PSO-PTS. Note that FTD-PTS reaches the optimal PAPR reduction performance when Q = 40. It can be concluded that FTD-PTS has a lower computational complexity than PSO-PTS to achieve better PAPR reduction performance.

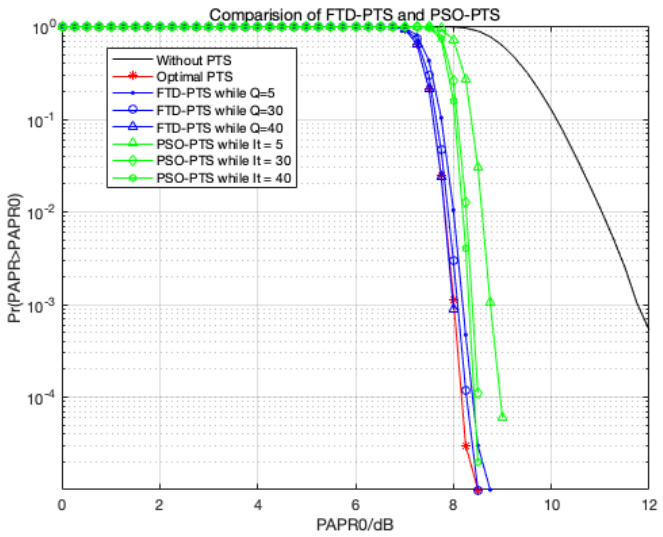

Figure 12. The performance comparison of FTD-PTS and PSO-PTS.

Table 7. PAPR reduction performance comparison of FTD-PTS and PSO-PTS.

PTS Schemes	PAPR Value When CCDF = 10^{-3}	PAPR Gain
Without PTS	11.5	0
FTD-PTS with Q = 5	8.3	3.2
FTD-PTS with Q = 30	7.9	3.6
FTD-PTS with Q = 40	7.7	3.8
PSO-PTS with Q = 5	8.9	2.6
PSO-PTS with Q = 30	8.3	3.2
PSO-PTS with Q = 40	8.2	3.3
Optimal PTS	7.7	3.8

7. Conclusions

This paper introduced two novel PTS techniques. F-PTS achieved a 91.8% optimal PAPR reduction performance (0.35 dB less) using 50% operation time compared to conventional PTS, which reduced the computational complexity of multiplier operations dramatically and maintained a compromise PAPR reduction performance.

FTD-PTS adopts a time- and frequency-domain joint evaluation algorithm and expands the candidate signal space for the dispersion evaluation. FTD-PTS improved by 18.7% the PAPR reduction performance (0.6 dB) compared to conventional PTS with a similar computational complexity, which reached the optimal PAPR reduction performance within a reasonable computational complexity and therefore can meet the demand of reducing PAPR in large data transmission systems.

Compared with other research results, the FTD-PTS algorithm improved PAPR reduction performance by 15.1% (0.45 dB) compared to PSO-PTS with a similar computational complexity.

In the future, further development of PAPR reduction schemes can be made in the following directions: enhancing the multicarrier system; redesigning the PAPR reduction schemes optimization objectives; combining artificial intelligence algorithm and PAPR reduction scheme.

Author Contributions: Conceptualization, F.H., Y.L. and L.J.; methodology, F.H., Y.L. and Z.X.; software, G.Z., J.X. and J.L.; validation, F.H., Y.L. and L.J.; formal analysis, F.H., Y.L., J.L. and L.J.; investigation, G.Z., J.X. and J.L.; resources, F.H., J.L. and L.J.; data curation, F.H. and Y.L.; writing—original draft preparation, F.H. and Y.L.; writing—review and editing, F.H., Y.L. and L.J.; visualization, F.H., Y.L. and L.J.; supervision, F.H., J.L. and L.J.; project administration, F.H., J.L. and L.J.; funding acquisition, F.H., J.L. and L.J. All authors have read and agreed to the published version of the manuscript.

Funding: This work was supported by "the Fundamental Research Funds for the Central Universities".

Institutional Review Board Statement: Not involved in relevant matters.

Informed Consent Statement: Not involved in relevant matters.

Data Availability Statement: Not involved in relevant matters.

Conflicts of Interest: The authors declare no conflict of interest. The funders had no role in the design of the study; in the collection, analyses, or interpretation of data; in the writing of the manuscript, or in the decision to publish the results.

Abbreviations

The following abbreviations are used in this manuscript:

Abbreviation	**Full Name**
PAPR	Peak-to-average power ratio
OFDM	Orthogonal frequency division multiplexing
PTS	Partial transmit sequence
SLM	Selective mapping
SMO	Spacing multiobjective
HPA	High-power amplifiers
BER	Bit error rate
CCDF	Complementary cumulative distribution function
Notations	**Interpretation**
$x(t)$	Continuous-time baseband OFDM signal
$X_k(t)$	Frequency-domain OFDM signal
x_n	Discrete-time baseband OFDM signal
$\mathbf{X}_v$	*V disjoint sub-blocks*
$X(k)$	Signals appears in the vth sub-blocks
$\mathbf{b}$	Phase weighting factors
$\mathbf{x}$	Scrambled serial time-domain signal
$\boldsymbol{F}_v^{-1}$	IFFT calculation
$\mathbf{b}_{\text{opt}}$	Optimum phase factors combination
C_{add}	Additive computational complexity
C_{mult}	Multiplicative computational complexity
CS_{add}	Additive computational complexity of PTS when applying M searching space
CS_{add}	Multiplicative computational of PTS when applying M searching space
R_{ab}	Correlation among two random signals
$\rho_{a,b}$	Correlation among two random signals $x_a^{'}$ and $x_b^{'}$
$\tilde{\mathbf{X}}$	Frequency signals after scrambling in F-PTS
S	Dispersion of F-PTS signal
$\widetilde{\mathbf{b}}_{\text{opt}}$	Scrambled signal combination with the best dispersion in F-PTS
C_{f-add}	Additive computational complexity of F-PTS scheme
C_{f-mult}	Multiplicative computational complexity of F-PTS scheme
$\boldsymbol{x}_m$	Signal of FTD-PTS
$\lvert x_m^c \rvert^2$	Power of FTD-PTS signal
$\widehat{\mathbf{X}}$	Candidate signals in the frequency domain
$Spacing(\boldsymbol{X}_i)$	Dispersion of FTD-PTS signal
$\widehat{\mathbf{b}}_{\text{opt}}$	Scrambled signal combination with the best dispersion in FTD-PTS
$\mathrm{C}_{FTD-add}$	Additive computational complexity of FTD-PTS scheme
$\mathrm{C}_{FTD-mult}$	Multiplicative computational complexity of FTD-PTS scheme

References

1. Yin, H.; Zhang, L.; Roy, S. Multiplexing URLLC Traffic Within eMBB Services in 5G NR: Fair Scheduling. *IEEE Trans. Commun.* **2021**, *69*, 1080–1093. https://doi.org/10.1109/TCOMM.2020.3035582.
2. Fernandes, M.A.; Loureiro, P.A.; Brandão, B.T.; Lorences-Riesgo, A.; Guiomar, F.P.; Monteiro, P.P. Multi-Carrier 5G-Compliant DML-Based Transmission Enhanced by Bit and Power Loading. *IEEE Photonics Technol. Lett.* **2020**, *32*, 737–740. https://doi.org/10.1109/LPT.2020.2994045.
3. Pasha, S.G.; Kohir, V.V. OFDM based DVB-T system implementation using MATLAB and HDL coder. In Proceedings of the 2017 International Conference on Computing Methodologies and Communication (ICCMC), Erode, India, 18–19 July 2017; pp. 256–261. https://doi.org/10.1109/ICCMC.2017.8282686.
4. Flores-Guridi, P.; Larroca, F. The ISDB-T multiplex frame pattern explained. In Proceedings of the 2017 IEEE URUCON, Montevideo, Uruguay, 23–25 October 2017; pp. 1–4. https://doi.org/10.1109/URUCON.2017.8171871.
5. Cai, B.; Liu, A.; Liang, X. Low-Complexity Partial Transmit Sequence Methods Using Dominant Time-Domain Samples for Multicarrier Faster-Than-Nyquist Signaling. *IEEE Access* **2019**, *7*, 121552–121564.
6. Liu, J.; Zhao, Y.; Yang, J.; Tang, X. Performance Analysis of IEEE 802.15.4g MR-OFDM with Frequency Offset. In Proceedings of the 2019 IEEE 19th International Conference on Communication Technology (ICCT), Xi'an, China, 16–19 October 2019; pp. 179–183. https://doi.org/10.1109/ICCT46805.2019.8947114.
7. Wan, Y.; Liu, B.; Ren, J.; Ullah, R.; Mao, Y.; Chen, S.; Zhang, H.; Han, S.; Song, X.; Nan, T.; et al. PAPR-Degraded Secure OFDM-WDM-PON Based on Chaotic Set-Partitioned SLM. *IEEE Photonics Technol. Lett.* **2021**, *33*, 1387–1390. https://doi.org/10.1109/LPT.2021.3120664.
8. Bulusu, S.S.K.C.; Shaïek, H.; Roviras, D. HPA Linearization for Next Generation Broadcasting Systems with Fast Convergence-Digital Predistortion. *IEEE Trans. Broadcast.* **2021**, *67*, 776–790. https://doi.org/10.1109/TBC.2021.3081925.
9. Tehrani, A.F.; Yeh, H.-G.; Kwon, S.-C. BER Performance of Space—Time Parallel ICI Cancellation of OFDM in MIMO Power Line Communications. *IEEE Syst. J.* **2021**, *15*, 1742–1752. https://doi.org/10.1109/JSYST.2020.2968542.
10. Pundir, V.; Ahmad, A. Analysing the effect of modulation schemes and subcarriers on PAPR influence of Hybrid combination of Selective Mapping, Partial Transmit Sequence and Clipping. In Proceedings of the 2020 Research, Innovation, Knowledge Management and Technology Application for Business Sustainability (INBUSH), Greater Noida, India, 19–21 February 2020; pp. 35–38. https://doi.org/10.1109/INBUSH46973.2020.9392121.
11. Zhang, S.-Y.; Shahrrava, B. A SLM Scheme for PAPR Reduction in Polar Coded OFDM-IM Systems without Using Side Information. *IEEE Trans. Broadcast.* **2021**, *67*, 463–472. https://doi.org/10.1109/TBC.2020.3039696.
12. Nema, L.; Gupta, V. PAPR Reduction of Massive 5G Systems using Modified PTS with DCT Scheme. In Proceedings of the 2020 IEEE International Conference for Innovation in Technology (INOCON), Bangalore, India, 6–8 November 2020; pp. 1–5. https://doi.org/10.1109/INOCON50539.2020.9298366.
13. Ali, T.H.; Hamza, A. A novel combined SLM-PTS technique based on Genetic Algorithms for PAPR reduction in OFDM systems. In Proceedings of the 2020 Second International Conference on Embedded and Distributed Systems (EDiS), Oran, Algeria, 3 November 2020; pp. 71–75. https://doi.org/10.1109/EDiS49545.2020.9296434.
14. Tu, Y.-P.; Wu, F.-H.; Huang, Y.-F. A Novel Turbo Scheme Combining PTS with Adaptive TR for PAPR Reduction in OFDM Systems. In Proceedings of the 2020 International Symposium on Computer, Consumer and Control (IS3C), Taichung, Taiwan, 18–20 June 2020; pp. 122–125. https://doi.org/10.1109/IS3C50286.2020.00039.
15. Hu, M.; Wang, W.; Cheng, W.; Zhang, H. Initial Probability Adaptation Enhanced Cross-Entropy-Based Tone Injection Scheme for PAPR Reduction in OFDM Systems. *IEEE Trans. Veh. Technol.* **2021**, *70*, 6674–6683. https://doi.org/10.1109/TVT.2021.3078736.
16. Wang, M. A Low-Complexity Hybrid Subblock Segmentation PTS Scheme for PAPR Reduction in MIMO-OFDM System. In Proceedings of the 2020 IEEE 4th Information Technology, Networking, Electronic and Automation Control Conference (ITNEC), Chongqing, China, 12–14 June 2020; pp. 224–228. https://doi.org/10.1109/ITNEC48623.2020.9085147.
17. Wang, H.; Ma, X.; Zhang, Z. The Performance of the OFDM System's PAPR of Different Segmentation of PTS. In Proceedings of the 2009 International Conference on Environmental Science and Information Application Technology, Wuhan, China, 4–5 July 2009; pp. 511–514. https://doi.org/10.1109/ESIAT.2009.20.
18. Jiang, T.; Wu, Y. An Overview: Peak-to-Average Power Ratio Reduction Techniques for OFDM Signals. *IEEE Trans. Broadcast.* **2008**, *54*, 257–268. https://doi.org/10.1109/TBC.2008.915770.
19. Vijayalakshmi, M.; Reddy, K.R. Partial PSO-PTS based PAPR reduction in MIMO OFDM. In Proceedings of the 2017 IEEE International Conference on Power, Control, Signals and Instrumentation Engineering (ICPCSI), Chennai, India, 21–22 Sepember 2017; pp. 1246–1251. https://doi.org/10.1109/ICPCSI.2017.8391909.
20. Lu, H. A Section Theorem in Topological Ordered Spaces and its Applications to the Existence of Pareto Equilibria for Multi-objective Games. In Proceedings of the 2009 International Joint Conference on Artificial Intelligence, Hainan, China, 25–26 April 2009; pp. 3–6. https://doi.org/10.1109/JCAI.2009.14.
21. Li, B.; Xue, X.; Feng, S.; Xu, W. Layered Optical OFDM With Adaptive Bias for Dimming Compatible Visible Light Communications. *J. Light. Technol.* **2021**, *39*, 3434–3444. https://doi.org/10.1109/JLT.2021.3067495.
22. Yu, P.; Jin, S. An enhanced TKM-TR method for PAPR reduction of OFDM signals with peak regrowth and peak residual reduced. In Proceedings of the 2016 8th IEEE International Conference on Communication Software and Networks (ICCSN), Beijing, China, 4–6 June 2016; pp. 145–148, https://doi.org/10.1109/ICCSN.2016.7586636.

23. Liu, K.; Liu, Y. Adjustable Nonlinear Companding Transform Based on Scaling of Probability Density Function for PAPR Reduction in OFDM Systems. *IEEE Trans. Broadcast.* **2021**, *67*, 524–537. https://doi.org/10.1109/TBC.2021.3051520.
24. Hu, M.; Wang, W.; Cheng, W.; Zhang, H. A Generalized Piecewise Linear Companding Transform for PAPR Reduction in OFDM Systems. *IEEE Trans. Broadcast.* **2020**, *66*, 170–176. https://doi.org/10.1109/TBC.2019.2909183.
25. Hameed, L.S. A combined weighting and PTS technique for PAPR reduction in OFDM signals. In Proceedings of the Second International Conference on Current Trends in Engineering and Technology—ICCTET 2014, Coimbatore, India, 8 July 2014; pp. 228–232. https://doi.org/10.1109/ICCTET.2014.6966292.
26. Ni, C.; Jiang, T.; Meng, D.; Huang, B. Weighted distortion-to-signal ratio based PTS scheme in nonlinear distorted OFDM systems. In Proceedings of the 2014 IEEE/CIC International Conference on Communications in China (ICCC), Shanghai, China, 13–15 October 2014; pp. 349–353. https://doi.org/10.1109/ICCChina.2014.7008300.
27. Wang, L.; Yang, X.; Wang, Y. PTS scheme with low complexity IFFTs for PAPR reduction in SISO/MIMO OFDM. In Proceedings of the 2013 IEEE 4th International Conference on Electronics Information and Emergency Communication, Beijing, China, 15–17 November 2013; pp. 181–184. https://doi.org/10.1109/ICEIEC.2013.6835482.
28. Heo, S.; Joo, H.; No, J.; Lim, D.; Shin, D. Analysis of PAPR reduction performance of SLM schemes with correlated phase vectors. In Proceedings of the 2009 IEEE International Symposium on Information Theory, Seoul, Korea, 28 June–3 July 2009; pp. 1540–1543. https://doi.org/10.1109/ISIT.2009.5205837.
29. Pham, M.-T.; Zhang, D.; Koh, C.S. Multi-Guider and Cross-Searching Approach in Multi-Objective Particle Swarm Optimization for Electromagnetic Problems. *IEEE Trans. Magn.* **2012**, *48*, 539–542. https://doi.org/10.1109/TMAG.2011.2173559.